Mode Locking of Spin Waves Excited by Direct Currents in Microwave Nano-oscillators

S. M. Rezende, F. M. de Aguiar, R. L. Rodríguez-Suárez, and A. Azevedo
Departamento de Física, Universidade Federal de Pernambuco, Recife, PE 50670-901, Brazil
(Received 29 September 2006; published 21 February 2007)

A spin-wave theory is presented which explains the frequency pulling and mode locking observed when two closely spaced spin-transfer nanometer-scale oscillators with slightly different frequencies are separately driven in the same magnetic thin film by spin-polarized carriers at high direct-current densities. The theory confirms recent experimental evidence that the origin of the phenomena lies in the nonlinear interaction between two overlapping spin waves excited in the magnetic nanostructure.

DOI: 10.1103/PhysRevLett.98.087202 PACS numbers: 75.75.+a, 05.45.Xt, 75.30.Ds, 85.75.−d

A high-density spin-polarized direct current may critically excite spin waves (SWs) in a ferromagnetic thin metal film, due to a torque induced by the carrier spin on the film magnetization. This dynamical effect was predicted ten years ago independently by Berger [1] and Slonczewski [2], and has been intensively investigated ever since. Initially, signatures of SW excitation featured in transport measurements with point contacts onto metallic magnetic multilayers [3–6] were attributed to the so-called spin-transfer-induced (STI) torque. Lately, several authors [7–11] reported unambiguous observations of microwave frequency oscillations resulting from the precession of the magnetization driven by direct currents. The observed dependence of the oscillation frequency on the driving current has been successfully explained by nonlinear SW theory [12–14].

Raising the expectations for application of spin-torque nano-oscillators (STNOs) in wireless communication technology, recent experiments [15,16] have been reported in which two separate nanocontacts in close proximity are fed independently by two current sources, one for each contact. For certain well-defined current intervals in the post-threshold regime, the two microwave oscillations thus generated may phase lock. The observed spectra exhibit higher power and narrower peaks in the phase-locking regime [15,16]. Pufall and coworkers [17] have shown that phase locking is suppressed when the magnetic mesa between the contacts is cut with a focused-ion beam. These elegant experiments have demonstrated unequivocally that SWs play a prominent role in the coupling mechanism of the two STNOs. To our knowledge, all experiments on phase-locked STNOs hitherto reported in the literature employ out-of-plane magnetized multilayers, an inadequate configuration for applications because it requires large magnetic fields. In addition, the out-of-plane configuration has a difficult theoretical interpretation, because the internal magnetic field is highly nonuniform, so that the normal modes of the spin excitations are not plane waves [13,14,18]. In this Letter, a nonlinear SW theory is presented for two interacting in-plane magnetized STNOs, a more adequate configuration for which no external magnetic field is actually necessary. We predict frequency pulling and phase locking, similar to the ones observed in [15–17].

For completeness, let us briefly review the model magnetization dynamics in a single isolated STNO [13]. The Hamiltonian for the magnetic system in the nanocontacted film (thickness d) includes Zeeman, volume anisotropy of crystalline or shape origin, volume exchange, interlayer exchange, surface anisotropy, and dipolar contributions. The mechanism of driving is that proposed by Slonczewski [2] for a direct current flowing perpendicularly to the plane of a magnetic multilayer with intercalated ferromagnetic and nonmagnetic metallic thin films. In the region of each contact the time derivative of the spin angular momentum $\hbar\vec{S}$ can be seen as being caused by an effective torque, so that the STI driving is associated to an effective magnetic field acting on the magnetization of the film, given by $\vec{H}_{\mathrm{STI}} = (\beta J/\gamma S)\hat{z} \times \vec{S}$, where $\beta = \varepsilon\hbar\gamma/2dM_S e$, J is the electric current density traversing the film in the perpendicular direction and assumed to be uniform in the contact region, $\gamma = g\mu_B/\hbar$ is the gyromagnetic ratio, g is the spectroscopic factor, μ_B is the Bohr magneton, e is the electron charge, M_S is the saturation magnetization, $\hat{z}$ is the direction of the spin polarization, which is determined by the applied field that magnetizes the film, and ε is a spin-transfer efficiency parameter [2], that depends on the materials of the multilayer.

The various contributions can be expanded in terms of classical SW variables c_k and c_k^* through a series of transformations [13]. In the linear approximation, the resulting equation of motion for the SW variable c_k is $dc_k/dt = -i\omega_k c_k - (\eta_k - \beta J)c_k$, where ω_k is the frequency of the SW mode with wave number k and η_k is the corresponding phenomenological relaxation rate. Thus, the essential feature of the STI field is that it exerts a torque on the magnetization that tends to deviate it away from equilibrium, producing an effect opposite to that of the relaxation and effectively driving its motion. As a result, when the current density exceeds the critical value $J_c = \eta_k/\beta$, the SW mode supported by the film exponentially grows in amplitude, corresponding to a precession of the magneti-

zation vector about the equilibrium direction with increasing cone angle. The saturation process and the frequency shift observed experimentally at higher currents are governed by nonlinear effects [12–14]. The important contributions arise from three sources: the reduction in the STI torque due to the deviation of the magnetization from the equilibrium direction, the surface dipolar energy (demagnetizing effect), and the surface anisotropy energy. The full equation of motion, including the four-wave interactions in the perturbative approach, may be written as [13]

$$\frac{dc_k}{dt} = -i\omega_k c_k - (\eta_k - \beta J)c_k - iT_k\alpha_k n_k c_k - \frac{3\beta J}{2NS}(u_k^2 + v_k^2)n_k c_k, \quad (1)$$

where $n_k = c_k^* c_k$ is the SW population, u_k and v_k are the coefficients of the underlying Bogoliubov transformation, N is the number of spins S in the sample, and α_k is a numerical factor of order unity [13]. The nonlinear interaction parameter $T_k = -3\gamma\pi(M_{\rm eff} - M_S kd/2)/4NS$, where the effective magnetization is defined by $4\pi M_{\rm eff} = 4\pi M_S + H_S$, and H_S is the surface anisotropy field. Equation (1) shows that for $J > J_c$, as n_k increases and approaches NS, the STI driving decreases and its effect is balanced by the relaxation, so that the SW amplitude saturates. On the other hand, the effect of the nonlinear term is to shift the SW frequency downwards as n_k increases with increasing current, thus allowing the tunability of the STNOs.

Consider now that two closely spaced nanocontacts are made on the film, through which currents I_1 and I_2 flow into the film with uniform current densities J_1 and J_2, as schematized in Fig. 1. The spin-polarized electron flows excite standing SW modes 1 and 2, each with maximum amplitude in the center region of the corresponding current

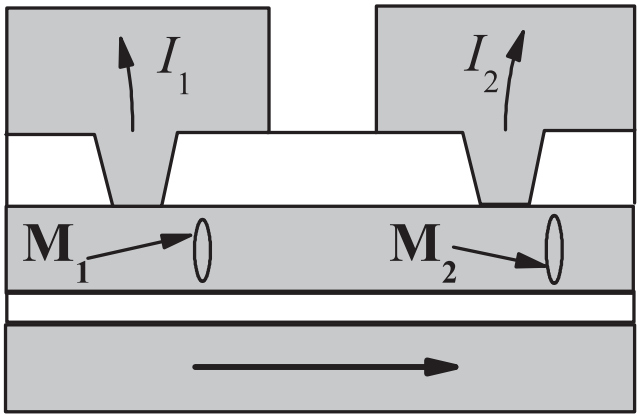

FIG. 1. Schematic representation of the cross section of two closely spaced spin-transfer nanometer-scale oscillators. The current direction is that for positive carriers. The horizontal arrow represents the pinned magnetization of an exchange-biased ferromagnetic underlayer.

flow. As shown in Ref. [17], the phase locking between the two oscillators is eliminated when the mesa between contacts is cut with a focused ion beam. Therefore, we assume that the SW mode in each contact overlaps with the one driven at the other contact, thus providing a mechanism for the mode coupling. As a result, in the region of each contact the local spin deviation is due to additive contributions of (i) the SW mode excited in that very region and (ii) a fraction λ of the amplitude of the mode driven in the other contact. This is taken into account by replacing c_i by $c_i + \lambda c_i$ ($i, j = 1, 2$; $i \neq j$) in the interaction terms. We then obtain the following equations of motion for the coupled system:

$$\frac{dc_1}{dt} = -i\omega_1 c_1 - (\eta_1 - \beta_1 J_1)c_1 - iT_1\alpha_1 n_1 c_1 - \frac{3\beta_1 J_1}{2SN} \times (u_1^2 + v_1^2)n_1 c_1 - i\frac{2}{3}T_1\lambda^2(\delta_1 n_2 c_1 + \delta c_1^* c_2 c_2) - \frac{\beta_1 J_1}{SN}\lambda^2[2(u_2^2 + v_2^2)n_2 c_1 + u_2^2 c_1^* c_2 c_2], \quad (2)$$

where

$$\delta_1 = 8(u_1^2 + v_1^2)(u_2^2 + v_2^2) + 16u_1 v_1 u_2 v_2 - 12(u_1^2 + v_1^2)u_2 v_2 - 12(u_2^2 + v_2^2)u_1 v_1 \quad (3)$$

and

$$\delta = 16u_1 v_1 u_2 v_2 + 4u_1^2 u_2^2 + 4v_1^2 v_2^2 - 6(u_1^2 + v_1^2)u_2 v_2 - 6(u_2^2 + v_2^2)u_1 v_1. \quad (4)$$

The equations for mode 2 are obtained from (2)–(4) by switching the subscripts 1 and 2. The real and imaginary parts of Eq. (2) and the corresponding ones for mode 2 constitute a set of four coupled nonlinear equations that are solved numerically, assuming that the driving currents I_1 and I_2 are applied to the contacts at instant $t = 0$ and that the initial conditions for the SWs are those of thermal equilibrium.

We apply our model equations to the following magnetic multilayer structure: two 4 nm-thick Permalloy (Py = $Ni_{80}Fe_{20}$) layers separated by a 8 nm-thick Cu layer, the top one being the free layer and the other one having magnetization pinned by the anisotropic exchange interaction with an antiferromagnetic underlayer. This multilayer is the same used by Krivorotov *et al.* [10] in experiments with only one STNO, but here we assume that it has two closely spaced contacts to apply the driving currents with densities J_1 and J_2 through the free layer. The advantage of this structure over the ones used in [15–17] is that it needs no external field for magnetizing the films in the plane. The following parameters obtained from Ref. [10] are used in the calculations: Applied field $H_0 = 0$, $d = 4$ nm, $I_c = 1.25$ mA, $4\pi M_{\rm eff} = 8.1$ kG, and $g = 2.0$. We assume that the SW mode excited by the current J_1 has critical current, frequency, and relaxation rate as observed in Ref. [10], namely $I_{c1} = 1.25$ mA, $\omega_1 = 2\pi \times 4.275$ GHz, and

$\eta_1 = 2.0\ \mathrm{ns}^{-1}$. Considering $4\pi M_s = 10.0$ kG as appropriate for Py, from the value of the frequency we determine the effective field $H_{\mathrm{AEK}} = H_{\mathrm{An}} + H_E + H_k = 0.278$ kOe, where H_{An}, H_E, and H_k are, respectively, the in-plane anisotropy field, the exchange field, and the contribution of the k-dependent terms in the frequency equation [13]. With these parameters we determine the coefficients of the SW mode, $u_1 = 1.385$, $v_1 = 0.958$, $\alpha_1 = 1.099$, and $T_1 NS = -24.8\ \mathrm{ns}^{-1}$. For the SW mode 2 excited by J_2 we assume $\omega_2 = 1.04 \times \omega_1 = 2\pi \times 4.446$ GHz, $T_2 = T_1$, $\eta_2 = \eta_1$, and $\beta_2 = \beta_1$ so that $I_{c2} = I_{c1} = I_c$, and the calculated coefficients are $u_2 = 1.367$, $v_2 = 0.933$, and $\alpha_2 = 1.107$. With these parameters we obtain a current dependence for the frequency of mode 1, isolated from mode 2 ($\lambda = 0$), in close agreement with the measurements reported in Ref. [10], exhibiting the downward frequency shift with increasing current (redshift), characteristic of experiments for the case of film magnetized in the plane. Thus, if the current at contact 1 is fixed at some value I_1, the frequency of mode 2 approaches that of mode 1 as I_2 increases in some range $I_2 > I_1$. The microwave frequency signals emitted by the oscillators are proportional to the rf components of the precessing magnetizations. Thus, we represent them by the normalized variables $a_i = \mathrm{Re}c_i/(NS)^{1/2} (i = 1, 2)$, which are proportional to the in-plane rf components of the magnetizations [13].

The bottom panel in Fig. 2 shows the calculated frequencies of the two oscillators for fixed driving currents $I_1 = 1.5I_c$ and $I_2 = 1.6I_c$, in the full range of coupling parameter $0 \leq \lambda^2 \leq 1$. The upper and middle panels show the trajectories in the phase plane a_2 vs a_1 and the spectra of $a_1 + a_2$ for three values of λ^2, corresponding to the solid symbols in the lower panel. The power spectrum is the square of the Fourier transform of $a_1 + a_2$, representing the spectrum of the signal in a power combiner with input signals proportional to a_1 and a_2. The trajectories a_2 vs a_1 give information on the relative amplitudes and phases of the two oscillations. Figure 2 unveils three coupling regimes, namely: *weak*, which, for the currents considered, is in the range $0 \leq \lambda^2 \leq 0.43$; *intermediate*, for $0.43 \leq \lambda^2 \leq 0.85$; and *strong*, for $0.85 \leq \lambda^2 \leq 1.0$. In the weak coupling regime, as λ^2 increases the two frequencies shift upwards and tend to approach each other. The shifts and the frequency pulling are produced by the nonlinear interaction represented by the fifth term in Eq. (2). In this regime the spectra display two distinct peaks and there is no correlation between the phases of the oscillations, as shown in the mid and upper panels for $\lambda^2 = 0.05$. As λ^2 reaches 0.43 the two frequencies jump to the same value and phase locking occurs. The single frequency spectrum and phase-locked trajectory, shown for $\lambda^2 = 0.5$, are the main features of the whole intermediate coupling range. As λ^2 increases further and enters in the strong coupling range, mode 1 is suddenly suppressed at $\lambda^2 = 0.85$ and the frequency jumps to the value for mode 2, as shown in Fig. 2 for $\lambda^2 = 0.90$. The mode suppression is a result of the nonlinear contribution to the damping of one mode by the increasing amplitude of the other mode, represented by the last term of Eq. (2). In actual experiments the value of the coupling parameter can be changed by varying the distance between the contacts. In a given structure λ^2 is fixed but one can investigate the effect of the coupling between the oscillators by varying the currents [15–17].

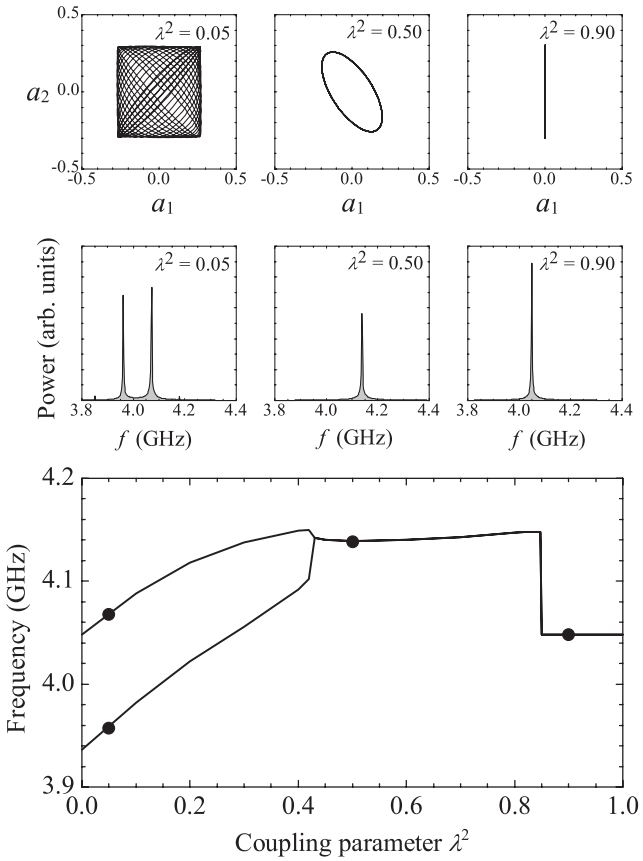

FIG. 2. Lower panel: Curves represent the frequencies of the two STI oscillators calculated for fixed driving currents $I_1 = 1.5I_c$ and $I_2 = 1.6I_c$, and varying coupling parameter λ^2. Symbols point out the values $\lambda^2 = 0.05$, 0.50, and 0.90 for which the trajectories in the phase plane a_2 vs a_1 in the upper panel and the spectra in the middle panels are calculated. The variables a_k defined by $a_k = \mathrm{Re}c_k/(NS)^{1/2}$ are proportional to the in-plane rf components of the magnetizations.

Figure 3 shows results obtained with $\lambda^2 = 0.50$, fixed current $I_1 = 1.5I_c$, and varying I_2. In the range $1.5I_c < I_2 < 1.575I_c$ the spectra show two distinct peaks and the two modes are unlocked, as seen in the a_2 vs a_1 map for $I_2 = 1.54I_c$. As I_2 increases in this range the frequency of mode 2 decreases due to the redshift and the frequency of mode 1 increases due to the pulling. As I_2 increases further and enters in the range $1.575I_c < I_2 < 1.712I_c$, the modes lock at a frequency intermediate between the two frequencies, as shown in the mid and upper panels for $I_2 = 1.70I_c$.

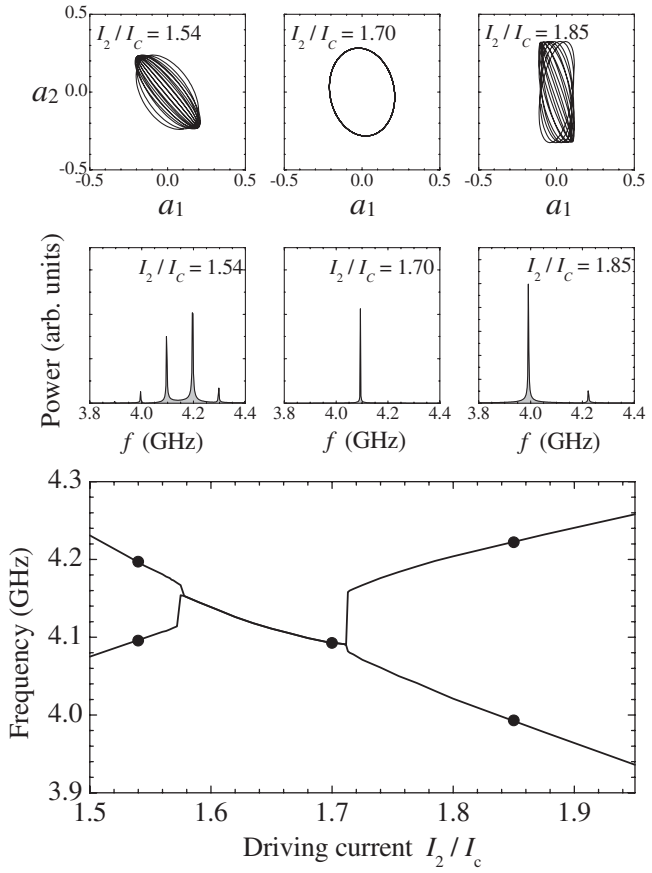

FIG. 3. Bottom panel: Solid lines represent the frequencies of the two STI oscillators calculated for fixed coupling parameter $\lambda^2 = 0.50$, fixed driving current, $I_1 = 1.5 I_c$, and varying current I_2. The upper and middle panels show the trajectories in the phase plane a_2 vs a_1 and the corresponding power spectra of $a_1 + a_2$, for $I_2/I_c = 1.54$, 1.70, and 1.85. These regimes are indicated by the solid circles in the bottom panel.

For $I_2 > 1.712 I_c$ the modes unlock, the frequency of mode 2 still decreases with increasing I_2, while that of mode 1 increases due to a frequency pushing effect caused by the fifth term in Eq. (2).

In sum, it is shown that a spin-wave theory incorporating nonlinear interactions predicts frequency pulling or pushing and mode locking when two STNOs with slightly different frequencies are separately driven in the same in-plane magnetized thin film by spin-polarized carriers at high direct-current densities. The results qualitatively agree with recent experiments with a magnetic field nearly perpendicular to the sample plane, and challenge further research using in-plane magnetized samples, since it is more adequate for applications. Because of the anisotropic propagation of SWs in thin films magnetized in the plane, we stress that the two contacts must be along a direction perpendicular to the magnetization, so that the SW generated in one contact propagates in the direction of the other one.

This work is supported by the Brazilian agencies CNPq, CAPES, FINEP, and FACEPE.

Note added in proof.—After submission of the manuscript of this Letter we learned of recent theoretical papers on coupling and mode locking of STNOs [19–21].

[1] L. Berger, Phys. Rev. B **54**, 9353 (1996).
[2] J. C. Slonczewski, J. Magn. Magn. Mater. **159**, L1 (1996); **195**, L261 (1999).
[3] M. Tsoi, A. G. M. Jansen, J. Bass, W.-C. Chiang, M. Seck, V. Tsoi, and P. Wyder, Phys. Rev. Lett. **80**, 4281 (1998).
[4] E. B. Myers, D. C. Ralph, J. A. Katine, R. N. Louie, and R. A. Buhrman, Science **285**, 867 (1999).
[5] W. H. Rippard, M. R. Pufall, and T. J. Silva, Appl. Phys. Lett. **82**, 1260 (2003).
[6] Y. Ji, C. L. Chien, and M. D. Stiles, Phys. Rev. Lett. **90**, 106601 (2003).
[7] S. I. Kiselev, J. C. Sankey, I. N. Krivorotov, N. C. Emley, R. J. Schoelkopf, R. A. Buhrman, and D. C. Ralph, Nature (London) **425**, 380 (2003).
[8] W. H. Rippard, M. R. Pufall, S. Kaka, S. E. Russek, and T. J. Silva, Phys. Rev. Lett. **92**, 027201 (2004).
[9] S. I. Kiselev, J. C. Sankey, I. N. Krivorotov, N. C. Emley, M. Rinkoski, C. Perez, R. A. Buhrman, and D. C. Ralph, Phys. Rev. Lett. **93**, 036601 (2004).
[10] I. N. Krivorotov, N. C. Emley, J. C. Sankey, S. I. Kiselev, D. C. Ralph, and R. A. Buhrman, Science **307**, 228 (2005).
[11] Q. Mistral, J.-V. Kim, T. Devolder, P. Crozat, C. Chappert, J. A. Katine, M. J. Carey, and K. Ito, Appl. Phys. Lett. **88**, 192507 (2006).
[12] S. M. Rezende, F. M. de Aguiar, and A. Azevedo, Phys. Rev. Lett. **94**, 037202 (2005).
[13] S. M. Rezende, F. M. de Aguiar, and A. Azevedo, Phys. Rev. B **73**, 094402 (2006).
[14] A. Slavin and P. Kabos, IEEE Trans. Magn. **41**, 1264 (2005).
[15] S. Kaka, M. R. Pufall, W. H. Rippard, T. J. Silva, S. E. Russek, and J. A. Katine, Nature (London) **437**, 389 (2005).
[16] F. B. Mancoff, N. D. Rizzo, B. N. Engel, and S. Tehrani, Nature (London) **437**, 393 (2005).
[17] M. R. Pufall, W. H. Rippard, S. E. Russek, S. Kaka, and J. A. Katine, Phys. Rev. Lett. **97**, 087206 (2006).
[18] M. A. Hoefer, M. J. Ablowitz, B. Ilan, M. R. Pufall, and T. J. Silva, Phys. Rev. Lett. **95**, 267206 (2005).
[19] A. N. Slavin and V. S. Tiberkevich, Phys. Rev. B **72**, 092407 (2005).
[20] J. Grollier, V. Cros, and A. Fert, Phys. Rev. B **73**, 060409(R), (2006).
[21] A. N. Slavin and V. S. Tiberkevich, Phys. Rev. B **74**, 104401 (2006).